Journal of CO2 Utilization 51 (2021) 101642

Contents lists available at ScienceDirect

Journal of CO2 Utilization

journal homepage: www.elsevier.com/locate/jcou

Cold plasma-Metal Organic Framework (MOF)-177 breathable system for atmospheric remediation

Fnu Gorky [a], Apolo Nambo [b], Maria L. Carreon [a,*]

[a] Chemical and Biological Engineering Department, South Dakota School of Mines & Technology, 501 E Saint Joseph St, Rapid City, SD, 57701, USA
[b] Bert Thin Films, LLC, 625 Myrtle St, Louisville, KY, 40298, USA

ARTICLE INFO

Keywords:
Non-thermal plasma
Methane capture
Carbon dioxide capture
Metal organic framework
Methanol synthesis
Atmospheric remediation

ABSTRACT

The direct capture of CO_2 and CH_4 from the atmosphere to stabilize the concentrations in the air to control global warming is accelerating. There are continued efforts to develop and optimize different technologies for capture and sequestration of these greenhouse gases from industrial emission sites. In this work we employed MOF-177 as an efficient CO_2 and CH_4 adsorbent at standard temperature and pressure conditions. We demonstrated the possibility of desorbing the gases under study when employing gentle plasma pulses of He. Moreover, we performed the synthesis of methanol from CH_4 using O_2 and CO_2 as oxidants respectively in the presence of MOF-177. We observed the highest conversion for the $CH_4 + O_2$ system when employing the MOF-177 at (5:1) (CH_4: O_2) flow ratio of 23.5 % and methanol selectivity of 17.65 %. While the best performance for the $CH_4 + CO_2$ system at the same conditions i.e., (5:1) (CH_4: O_2) flow ratio was 18.4 % for the methane conversion and 11.68 % for the selectivity towards methanol. We expect this preliminary understanding of the adsorption-reaction system under non-thermal plasma environment can lead to future atmospheric remediation technologies.

1. Introduction

The stabilization of CO_2 and CH_4 concentrations in the air to control global warming is accelerating. There are continued efforts to develop and optimize different technologies for capture and sequestration of these greenhouse gases from industrial emission sites. From these gases, CH_4 is the most dominant anthropogenic greenhouse gas (after CO_2). Methane can react with nitrogen oxides leading to tropospheric ozone pollution and posses a higher global warming potential (GWP) than CO_2. It is 84 times more potent than CO_2 over the first 20 years after release and ~28 times more potent after a century. Methane concentrations could be restored to preindustrial levels by removing ~3.2 of the 5.3 Gt of CH_4 currently in the atmosphere [1]. Rather than capturing and storing the methane, CH_4 could be oxidized to CO_2, through the thermodynamically favorable reaction:

$$CH_4 + 2O_2 \rightarrow CO_2 + 2H_2O;\ \Delta H_{rx} = -803\ kJ\ mol^{-1}.$$

With the possible production of valuable condensates such as formaldehyde and methanol when employing different reaction conditions (i.e., gas ratio, oxidant type, temperature) and rational selected catalysts. The large activation barrier associated with splitting methane's C—H bond (435 kJ mol–1/4.5 eV) and CO— in carbon dioxide (805 kJ mol-1/8.34 eV) could in principle be overcome by the sole use of non-thermal plasma (NTP) that has the advantages of low gas bulk temperature and possible pairing with renewable energy sources such as solar and wind. As a motivation to this work serves our extensive experience in non-thermal plasma catalytic ammonia synthesis [2–10] where only plasma when employing a DBD set up allows to overcome the high activation barrier associated with the N—N bond (941. 69 kJ/mol–1/9.75 eV).

In general, the thermal catalytic conversion of CH_4 is associated with several challenges that still need to be overcome, such as the high temperature for thermal activation of CH_4 at which several products decompose making essentially impossible to achieve high conversions and selectivities simultaneously, preventing high single pass product yields.

In non-thermal plasma environment, oxygen is known to be very effective for activation of methane. However, a possible drawback is the excessive oxidation which results in the formation of CO_2 and a variety of oxygenates. Hence, the use of CO_2 as a milder oxidant could be beneficial to achieve targeted desired products adding the benefit of chemically treating two of the most important green-house gases and

* Corresponding author.
E-mail address: Maria.CarreonGarciduenas@sdsmt.edu (M.L. Carreon).

https://doi.org/10.1016/j.jcou.2021.101642
Received 5 June 2021; Received in revised form 1 July 2021; Accepted 5 July 2021
Available online 14 July 2021

convert them into high value chemicals.

One of the most ambitious research efforts in recent years focuses on the direct capture of CH_4 from ambient air and other dilute sources. Most sorbents for such purpose rely on the use of materials with significant CH_4 affinity. The non-polarity of the CH_4 molecule results in a challenging weak interaction with most materials. Promising materials due to their rich chemistry composition include metal-organic frameworks (MOFs), zeolites, and covalent organic frameworks (COFs). Moreover, process intensification is currently of great interest to capture and convert CH_4 to value-added chemicals without requiring costly CH_4 transportation and storage.

In terms of electron stimulated desorption (ESD) previous relevant reports show that the desorption of CO_2 when using non-thermal plasma is more significant and rapid compared to thermal desorption. This when employing systems under similar conditions and electric power levels [11]. Recently, it has been reported that plasma is capable of desorbing CO_2 from a hydrotalcite surface, with the desorption starting instantly after plasma ignition. While desorption stopped when plasma is turned off, indicating a possible instant control of the process [12].

Herein, we present the evaluation of two different non-thermal plasma systems that have the main objective to serve as a seed for the future development of atmospheric plasma-remediation technology. We evaluated the mixtures CH_4/O_2 and CH_4/CO_2 with and without He dilution. Important differences between these two gas mixtures are the type of plasma generated, where the CH_4/O_2 plasma is more electronegative comprising the highest negative ion density which has resulted in an observed lower time-space electron density theoretically predicted compared to the CH_4/CO_2 plasma [13]. The selected low O_2 concentration with respect to CH_4 (5:1; CH_4:O_2) or (2.5:2.5:1; CH_4: O_2: He) was set based on the premise that higher O_2 fraction leads toward full oxidation of CH_4. The objective of this paper is to favor partial oxidation to improve the formation of condensates since it would be beneficial from an economic point of view. However, before the CH_4 and CO_2 can be reacted in plasma, they should be removed from air. The removal of CH_4 and CO_2 from air requires the use of suitable adsorbents with large selectivity and adsorption capacity. In this work we employed MOF-177. For adsorption purposes, zinc-based metal-organic frameworks (MOFs) are considered ideal due to their high specific surface area, tunable pore size and large accessible pore volume [14–16]. In fact, Yagui et al. [17] measured CO_2 adsorption in different Zn-based MOFs showing that MOF-177 can adsorb 35 mmol/g of CO_2 at 45 bar at room temperature.

While more recent computational studies [14] show that the adsorption equilibrium capacity of CO_2 and CH_4 on MOF-177 at 298 K are 39.69 wt % at 14 bar and 22.03 wt % at 100 bar respectively. In this work plasma catalytic results of methane oxidaxion when using CO_2 and O_2 as oxidants are presented. Moreover, to experimentally observe the desorption of CH_4 and CO_2 when a gentle plasma is applied, the MOF-177 was loaded with CH_4 and CO_2 at ambient conditions. The desorption of CH_4 and CO_2 was performed employing He plasma to avoid the use of highly reactive gases that can lead to the production of chemicals. The use of this noble gas allowed us to follow the CH_4 and CO_2 desorption through gas chromatography and emission spectra (OES) when employing subtle plasma disruptions.

2. Experimental methods

The MOF employed in this work is the commercially available, MOF-177. MOF-177 is a framework consisting of a $[Zn_4O_6]^{6+}$cluster and linker 1,3,5-benzenetribenzoate (BTB) ligands. MOF-177 (Basolite Z377, Sigma Aldrich) has the empirical formula: $C_{54}H_{30}O_{13}Zn_4$ and molecular weight of 1148.37. The chemical composition of MOF-177 is Carbon (C) 55 g/100 g, Zinc (Zn) 22 g/100 g ± 10 %. The BET surface area given by the provider ranges from 3800–4000 m^2/g. With a median pore diameter recorded in the microporous region between 10.6 A [18] and 12.7 A [19].

The temperature was measured using a Fluke (62 Max) IR thermometer for the two presented configurations (packed bed reactor) and plasma only (plug flow reactor). For accurate collection of the temperatures, the IR Thermometer was positioned at a safe distance of 5–7 inches away from the reactor consisting of quartz tube and ground electrode copper mesh. The collection was carried out meticulously at different times (0, 3, 6, …, 21 min) and at three different positions as presented in Fig. S1 and further averaged for consistency.

3. Characterization methods

Scanning electron microscopy images were collected on a Zeiss Supra40 variable-pressure field-emission operated at accelerating voltages of 1–3 kV. Before analysis, MOF-177 samples were gold sputter-coated for 2−3 min to preclude charging.

Surface area, pore size and pore volume were analyzed using the micromeritics Gemini II—2375 BET (Brunauer-Emmett-Teller) surface area analyzer. Fresh and spent (after 5 h of plasma exposure) MOF-177 samples were degassed at 200 °C for 8 h before analysis.

Powder X-ray diffraction patterns were collected on a 3rd generation Empyrean, Malvern Panalytical (Cobalt Source), operated at 45 mA, and 40 kV.

3.1. Reactor setup

The catalytic activity of the studied MOF-177 was evaluated in a custom designed Dielectric Barrier Discharge (DBD). The testing system can be divided in five main parts: 1) the reactor core, 2) the emission spectrum capture system (OES), 3) the electrical characterization set up (oscilloscope), 4) the cold trap and 5) the Gas Chromatograph. The complete set up is shown in Fig. 1. To perform the catalytic tests, CH_4 and O_2 and CH_4 and CO_2, respectively were connected to the reactor through mass flow controllers. The exit of the reactor was connected to a cold trap to condensate any of the oxygenates produced. While the exit of the cold trap is connected directly to the GC for online gas quantification. The quantification was performed using an Agilent 7820A GC equipped with a HP-PLOTU column (30 m ×0.32 mm ×10 μm) and hydrogen gas as carrier. The high voltage power supply was connected to the reactor using Litz wire and alligator clips. The inner electrode made of tungsten rod (2.4 mm diameter) was placed at the center of the quartz tube with an I.D. of 4 mm and O.D. of 6.40 mm. The fittings were made of PFA (PerFluoroAlkoxy) to avoid any arc formation. The outer electrode made of tinned copper mesh acted as the ground electrode. The length of the plasma zone was ~ 8 cm. The impedance of the chamber was matched to deliver maximum power. To achieve maximum power transfer from source to load, the load's impedance must match the characteristic impedance of the generator.

The gases flow through the annulus and two quartz frits were placed carefully such that they do not cause any pressure increase. And to avoid the displacement of the catalyst. 100 mg of MOF-177 were loaded as a fine powder in the reactor. The reaction mixture was flow to the reactor for 20 min after the reactor was sealed, to homogenize the reactor chamber before striking plasma. The plasma-catalyst intersection zone was approximately 6 cm long. The MOF was packed in the overlap area between the inner and outer electrodes. The reactions were carried out at the feed flow ratio of 5:1 CH_4 to O_2/CO_2 (CH_4: O_2/CO_2) or 2.5: 2.5:1 ratio of CH_4 to He to CO_2 (CH_4: He: CO_2) respectively with a total flow rate of 30 sccm at the applied voltage of 12.5 ± 0.5 $kV_{pk\text{-}pk}$. We kept the average bulk temperature of the reactor at the average value of 62 °C (±7.1 °C) with the use of a fan continuously running during the reaction time. The methanol selectivity here reported refers to the micromoles/min of methanol produced per the micromoles/min of limiting reactant converted. In this case CO_2 or O_2 respectively. To determine the methane conversion, the exhaust gas was sent to the gas chromatograph properly calibrated. Gas injections to the GC where performed every 10 min during the total reaction time of 300 min. The calibration curve details are provided in Table S1. The reactor was connected to an

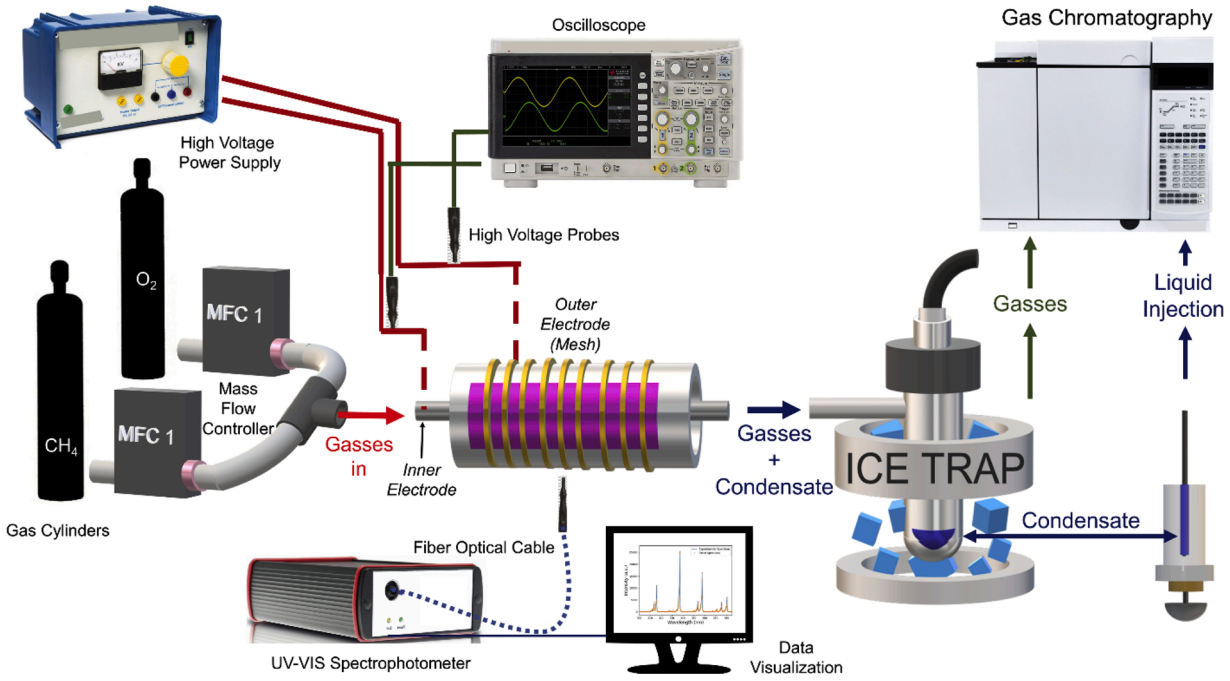

Fig. 1. Schematic of the Dielectric Barrier Discharge (DBD) reactor setup employed in this study.

oscilloscope to obtain the current and voltage waveforms. A Tektronix 2048 series oscilloscope was used along with a Tektronix P6015A high voltage probe having a 1000X voltage reducing rating. The current was measured by a 10X current reducing probe to get the waveforms. The energy delivered to the reactor was calculated based on these measurements.

The light emitted from the discharge was led through an optical system and the emission spectra of the glow region were measured at the center of the tube. The measurements were recorded using a dual channel UV–vis-NIR spectrophotometer in scope mode (Avantes Inc., USB2000 Series). The spectral range was from 200−1100 nm, using a line grating of 600 lines/mm and resolution of 0.4 nm. A bifurcated fiber optic cable with 400 μm was employed.

3.2. Plasma catalytic methane oxidation

When employing O_2 for the methane oxidation reaction in a DBD reactor in the absence of a catalyst (i.e., only plasma) the reported methane conversions range from 1.9 % to 7% and methanol selectivity ranging from 19 % to 47 % [20–23]. While there is an observed enhancement when adding a catalyst in the DBD reactor (plasma catalysis). Methane conversions are reported higher for this case, in the range of 9%–54.5%, while methanol selectivities fall in the 22.2–40% range [21,24–27]. (see state of the art Table S2). For the case of CO_2 as oxidant methane conversions range from 15.5 % to 47.5 % while the methanol selectivities from 0.2 % to 14 %. (see state of the art Table S2).

3.3. The MOF-177 stability when exposed to non-thermal plasma

Previous reports on MOF-177 stability showed that its structure remains intact at temperatures below 330 °C under a flow of oxygen but decomposes to zinc oxide at 420 °C [28]. In our case the reaction temperature was maintained at the average bulk temperature of 62 °C (±7.1 °C) during the 5 h of reaction. To experimentally observe the possible morphological changes in the MOF-177 due to the plasma exposure we performed SEM analysis before and after reaction. It can be observed in Fig. 2a that there is not a definite crystal shape observed as reported previously for this MOF [19,29]. Most probably due to the polycrystalline agglomerate nature of the crystals. Interestingly after plasma reaction with O_2 and CO_2 (Fig. 2b and c) the samples appearance change resembling the microcuboids reported by Li et al. at specific synthesis conditions [30]. But showing a dense appearance for the sample when the CH_4 was reacted with O_2 as an oxidant. When the sample reacted with CO_2 (Fig. 2c) there is a visible reduction in particle size when compared to fresh catalyst and O2 plasma spent catalyst (Fig. 2b and c).

As reported for other plasma catalysis reactions the area of the MOF is reduced by the collision of highly energetic particles from the plasma [4,31]. This is the case for the reaction $CH_4 + O_2$ where the surface area

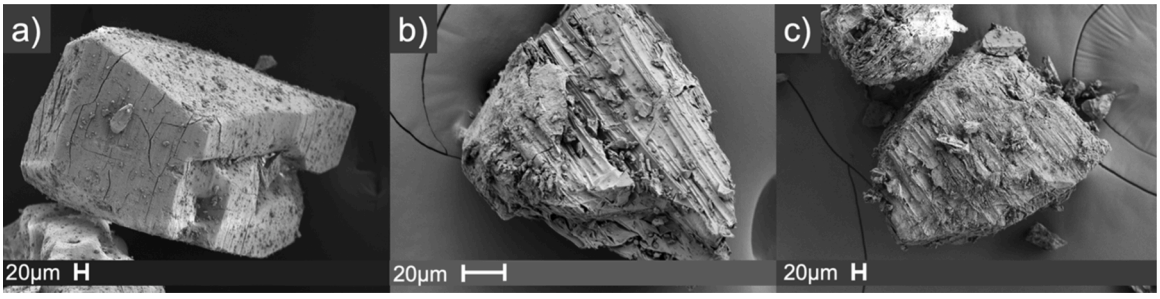

Fig. 2. SEM images of microporous crystals employed as catalysts in this study a) MOF-177 (Fresh), b) MOF-177 (Spent) (CH_4+O_2) after 300 min of reaction, c) MOF-177 (Spent) (CH_4+ CO_2) after 300 min of reaction.

of the catalyst gets reduced from 3354.2 $m^2\ g^{-1}$*(fresh)to 538.6* $m^2\ g^{-1}$ *(spent)* most probably due to damage to the linker. While for the case of the reaction $CH_4 + CO_2$ the plasma leads to a reduction in the particle size that results in an increase on the external surface area. The observed total surface area for the catalyst employed for the $CH_4 + CO_2$ changed from 3354.2 $m^2\ g^{-1}$*(fresh) to 3409.18* $m^2\ g^{-1}$ *(spent)*. We hypothesize that this observed behavior is due to the high affinity that the MOF-177 has for the CO_2 as reported before [14,17]. This affinity allows the CO_2 to diffuse in to the MOF-177 surface and pores freely transfering its reactivity in a uniform way avoiding damage to the linker but allowing the particle size reduction and the observed increase in the external surface area (Table 1).

The XRD data for the fresh sample MOF-177 and the spent samples after reaction with CH_4 and O_2 and CO_2 as oxidants respectively is presented in Fig. 3. The theoretical XRD data was take from the available literature [32]. The main peaks for this MOF-177 are identified at 4.7°, 6.2°, 10.1° and 13.5° according to Saha [33]. However, the XRD patterns presented by different groups differ to some extent. Li and Yang [29] reported that the largest peak appears around 5° while Rowsell [34] around 6°. There are also reported differences in the location of the smaller peaks. Probably due to the different crystallization conditions during the synthesis. In our case, when comparing the fresh MOF-177 sample versus the spent samples after reaction it is evident a slight displacement to the right that might be indicating the distortion of the crystalline structure after plasma reaction. In fact our group has reported this previously for Ni-MOF-74 when exposed to RF plasma [4]. In our previous reports on plasma ammonia synthesis when employing MOFs as catalysts we have observed that the structural stability depends on the plasma power. For the specific case of the Ni-MOF-74 we reported that high plasma powers, i.e., 300 W when using a low-pressure radio-frequency (RF) plasma discharge caused framework amorphization due to the collision of highly energetic species from the plasma [4]. In the atmospheric regime, when employing a Dielectric Barrier Discharge (DBD) we have observed that ZIF-8 displayed remarkable stability upon recycling during plasma catalytic ammonia synthesis [35] Interestingly, for this case at the diffraction angle of 6° emerges a trilateral peak compare to the theoretical single peak for MOF-177, which can be ascribed to the crystal lattice perturbation caused by the incarceration of the guest molecules into the pores of MOF-177 [18,32,36]. (Pictures of the MOF-177 fresh and spent can be seen in Fig. S2)

3.4. MOF-177 catalytic performance

The MOF-177 catalytic performance was measured in a DBD reactor at the average power of 7 W and frequency of 21,000 Hz (please refer to the electrical data in the supporting information, Fig. S3a,b). The total flow rate was 30 sccm. The reaction time was 300 min and all the reactions were run in triplicates. The explored flow ratios are shown in Fig. 4 where it can be observed that the O_2 as oxidant leads to higher CH_4 conversions and higher CH_3OH selectivities (Fig. 4a). The highest conversion for the $CH_4 + O_2$ system was observed for the MOF-177 at (5:1) (CH_4: O_2) flow ratio with a methane conversion value of 23.5 % and methanol selectivity of 17.65 %. While the best performance for the $CH_4 + CO_2$ system at the same conditions i.e., (5:1) (CH_4: O_2) flow ratio was

Table 1
Textural Properties of MOF-177 fresh vs spent (after 5 h of plasma reaction).

Catalyst	BET Surface Area ($m^2\ g^{-1}$)	Langmuir Surface Area ($m^2\ g^{-1}$)	Pore Volume ($cm^3\ g^{-1}$)
Fresh	3354.2	4714.5	1.70
Spent for sample using CO_2 as oxidant	3409.18	4793.75	1.74
Spent for sample using O_2 as oxidant	538.6	757.5	0.28

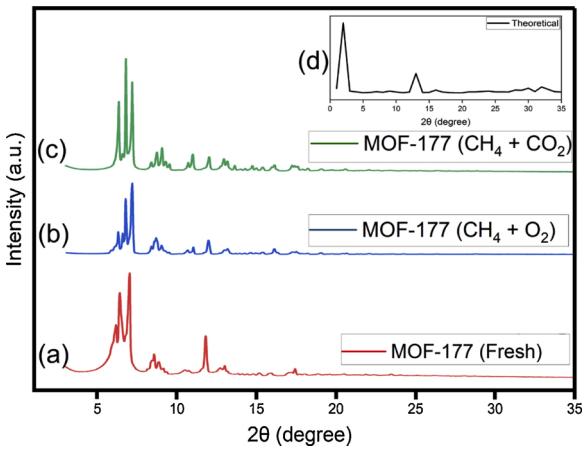

Fig. 3. XRD patterns showing (a) MOF-177 (fresh), (b) MOF-177 (Spent) after 5 h of reaction when using O2 as oxidant, (c) MOF-177 (Spent) after 5 h of reaction when using CO2 as oxidant and (d) MOF-177 theoretical take form [32].

18.4 % for the methane conversion and 11.68 % for the selectivity towards methanol (refer to Fig. 4b). The enhanced effect of the MOF-177 can be observed when comparing the only plasma vs the MOF-177 catalyzed reaction at same conditions i.e., (2.5:2.5:1) (CH_4: He: O_2/CO_2). For the $CH_4 + O_2$ system the methane conversion was at least 6 times greater with the MOF-177 than only plasma system. While for the $CH_4 + CO_2$ system the methane conversion was 12 times higher for the MOF-177 when compared to only plasma. This confirms the synergism non-thermal plasma-catalyst for both reaction systems. The oxygen system showed higher conversion and selectivity but had a great drop in surface area, suggesting that the reactive species are directed towards the linker and reagents. While the CO_2 system avoid damage to organic linker in MOF-177 the conversion and selectivity suffers a slight decreased when compared to O_2 which can suggest that the MOF has directing effect on CO_2 reactive species on the plasma-catalyzed system. The presented results show the evident benefit of coupling MOF-177 with non-thermal plasma. Where the conversions and selectivities are improved by the MOF presence. In fact, previous results on plasma catalysis for the $CH_4 + CO_2$ reaction when using UiO-67 MOF [37] showed that the MOF catalyst intensified the surface reactions in plasma improving the synergy capacity. To ascertain this for our MOF-plasma system the emission spectroscopic diagnostics was performed for the only plasma and the plasma-MOF system. As it can be observed in Fig. S4 the addition of the MOF changes the emission spectra. Specifically, the CO peaks (283 nm, 297 nm, 3rd positive system of CO) were constantly lower when the MOF is employed. This result can be associated with the high adsorption of reactive plasma species on the MOF surface. Which reduces the intensity in the spectra [38]. To evaluate the possible thermal effect, we have conducted additional experiments without plasma by using a heating tape surrounding the reactor core area. The temperature was maintained at the average value of 280 °C. This temperature was selected based on the thermal sensitivity of MOF-177 that decomposes around 330 °C [33]. After 5 h of reaction, there was no condensate formation i.e., no methanol was obtained. Moreover, this process is thermodynamically favored at high pressure as most literature on thermal catalysis have cited the use of 5–10 mPa [39] for the synthesis of methanol. Additionally, it was confirmed quantitatively with Gas chromatography with no additional peaks observed other than Methane and Carbon dioxide.

3.5. Plasma adsorption-desorption experiments on MOF-177

To observe the adsorption of CH_4 on the MOF-177. We passed CH_4 at a total flow rate of 25 sccm for 4 h. At STP conditions and when plasma off. This to allow the adsorption of CH_4 in the MOF. After 4 h, the CH_4

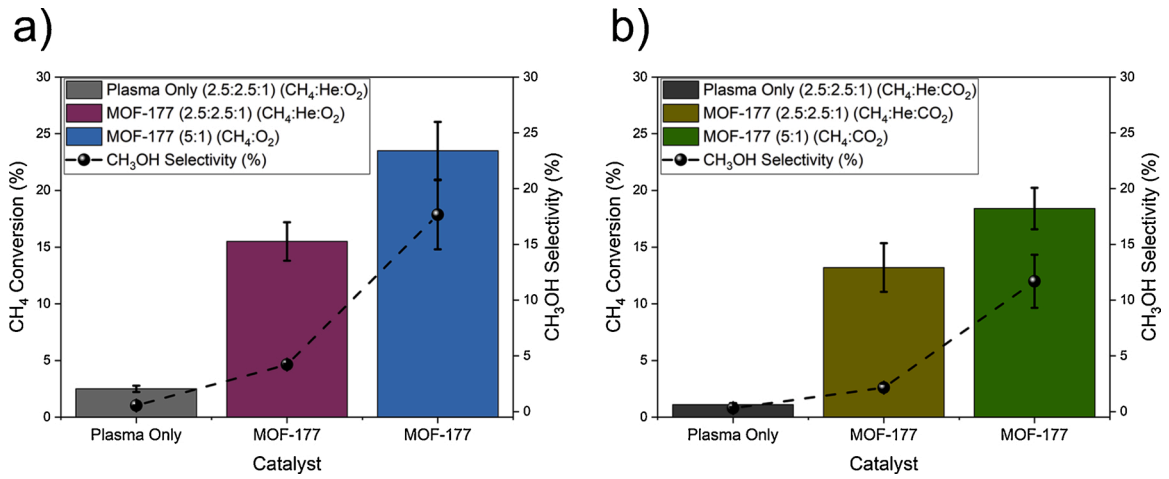

Fig. 4. Methane Conversion (%) Vs. Methanol Selectivity (%) with and without catalyst, a) for CH_4+O_2 & CH_4+He + O_2, b) for CH_4+CO_2 & CH_4+He + CO_2.

flow was completely stopped and 5 sccm of He were allowed in the chamber. Then the plasma was turned on at the low power of 4 W. Experiments were performed in triplicates. As it can be observed when the He plasma was turned on the CH_4 molar flow rate detected by the online GC increased. This behavior was repeatedly observed in pulses (see Fig. 5a). These results demonstrate the possibility of using plasma pulses to desorb the CH_4 adsorbed in the MOF. The maximum molar flow rate of CH_4 desorbed was 206.6 μmol min^{-1} at 122 min. The procedure was repeated for CO_2 separately. Since this MOF has been reported to adsorb both gases efficiently. The maximum molar flow rate of CO_2 desorbed was 195.09 μmol min^{-1}at 118 min. The OES analysis (Fig. 5c and d) show the presence of CH_4 and CO_2 active species confirmed in the gas phase at the adsorption conditions.

Aiming to understand the temperature effect on the desorption of CH_4 and CO_2. We have performed the plasma desorption using Krypton plasma to compare to Helium plasma desorption (see Fig. S5. Interestingly when using Kr plasma, the highest CH_4 desorption value was 187.3 μmol min^{-1}at 120 min, while for He was 206.6 μmol min^{-1} at 122 min. The average bulk temperature for the Kr plasma was measured to be 62 °C while for He plasma was 68 °C. For the case of CO_2, the highest desorption value was 190.5 μmol min^{-1} at 120 min at an average bulk temperature of 65 °C when using Kr plasma while the maximum value for He plasma was 195.09 μmol min^{-1} at 118 min at the average bulk temperature of 67 °C. In these experiments He leads to a higher average bulk temperature compare to Kr. And also to a higher desorbed amount of CO_2 and CH_4 compared to Kr. These results show the temperature effect in aiding in the desorption process. However, the effect of plasma can not be disregarded and more detailed experiments are needed to decouple the temperature and plasma effects. In terms of the benefits of using plasma it has been reported that NTP induced a greater amount of desorption of the adsorbed species that bonded strongly to the surface compare to simple heating [40]. Moreover, plasma showed a unique and precise control on desorption when turning on/off added to the possibility of using thermal sensitive materials such as MOFs.

The importance of these results resides in the possible development of a future plasma breathable MOF system. Where the CO_2 or CH_4 adsorbed in the MOF from the atmosphere will be desorbed by gentle plasma pulses using reactive mixtures. Allowing the easy desorption of captured gases from the atmosphere and their reaction to produce valuable oxygenates by subtle plasma disruptions.

Finally, if one compare to the traditional liquid amine systems for CO_2 absorption, the regeneration for this alternative method is an energy intensive process due to the high heat of sorption of CO_2 with amino groups and the high heat capacity of water present in these systems. All together incurring in high operating costs due to the high temperature required for such processes [41]. Moreover, the corrosive nature of such liquids could lead to a reinvestment for replacement or repair costs [42].

Beyond the economic point of view, such energy intensive processes have a greater carbon footprint and represent a high environmental hazard. Amine solutions for CO_2 capture very often release amine into the environment where it can be photo-oxidized forming compounds such as nitrosamines, nitramines and amides. These degradation products may cause carcinogenicity, mutagenicity and reproductive effects [41].

CO_2 solid sorbents generate less waste during recycling, are easier to handle, have less environmental precautions when disposed and lower energy requirements for regeneration [43,44]. The adsorption-desorption process can be done through changes in the pressure or temperature, which in the case of solid sorbents results in lower energy consumption due to the lack of large quantities of solvent and the lower heat capacities of solids [43].

4. Conclusions

Direct capture of CO_2 and CH_4 from air to stabilize their concentrations for global warming control is currently accelerating. Here in, we presented the possibility of employing non-thermal plasma to desorb and react these greenhouse gases. While much work still lies ahead this work intends to set up a proof of concept for this kind of intensified plasma systems. The MOF-177 employed resulted in a maximum CH_4 molar flow rate of 206.6 μmol min^{-1} when desorbed by a subtle plasma disturbance. While for CO_2 the maximum molar flow rate of CO_2 desorbed was 195.09 μmol min^{-1}. From the materials point of view, we were able to observe the influence of the oxidant over the catalyst employed, the more reactive oxygen species that lead to a higher methane conversion decreased the surface area by a factor of 6 while the CO_2 system increased slightly the catalyst surface area probably due to a reduction in particle size. The great impact of oxidant over the material opens a possibility of tunable plasma phase in order to obtain higher conversions with a longer catalyst life. Further studies on the different pathways of plasma methane oxidation would lead to a better system design where the material morphology and nature enhance the plasma properties and its effects on reactivity and propagation. Moreover, the low temperature plasma activation of CH_4 and CO_2 here used could lead to atmospheric plasma remediation technologies. While this work is just the starting point for a future intensified system, we expect this preliminary data improves our basic knowledge on a plasma adsorption-reaction system.

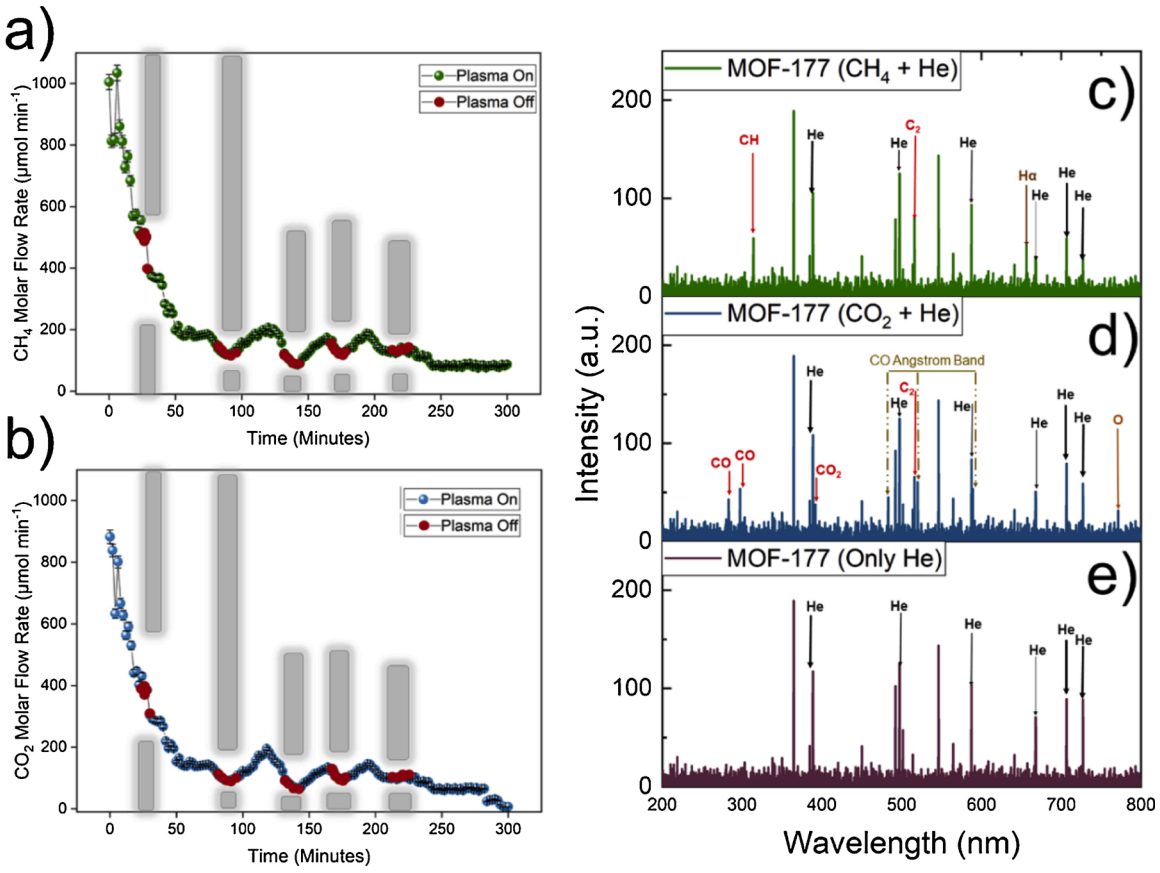

f)

Species	Wavelength (nm)	Transition	Reference
He I	388.6, 492.1, 501.5, 587.5, 667.8, 706.5, 728.1	2^3S-3^3P^0, 2^1P^0-4^1D, 2^1S-3^1P^0, 2^3P^0-3^3D, 2^1P-3^1D, 2^3P^0-3^3S, 2^1P^0-3^1S	[45]
C_2 (Swan system)	516	$A^3 \longrightarrow X^3$	[25,46,47]
CH band	314	$C^2 \longrightarrow X^2$	[25,46-48]
H_α	656.3	$3d^2D \longrightarrow 2p^2P$	[3]
CO	283, 297	3rd positive system of CO	[25,46,49]
CO Angstrom band	483,520,589	$B^1 \longrightarrow A^1$	[25,46,48]
O	777.1	$3s^5S^0 \longrightarrow 3p^5P$	[25,46,48]

Fig. 5. Plasma desorption when employing MOF-177 for a) Methane and b) Carbon Dioxide, c) OES for Methane + Helium, d) OES for Carbon Dioxide + Helium, e) OES for only Helium, f) summary of important plasma species [45,25,46,47,25,46–48,3,25,46,49,25,46,48,25,46,48].

Author contributions

Maria L. Carreon conceived the idea, directed the plasma catalytic synthesis experiments, as well as plasma desorption experiments and contribute to the writing of the manuscript. Fnu Gorky, performed the plasma experiments and collected the reaction data. Apolo Nambo helped with discussion for manuscript writing.

Declaration of Competing Interest

The authors declare that they have no known competing financial interests or personal relationships that could have appeared to influence

the work reported in this paper.

Acknowledgement

Maria L. Carreon thanks NSF-CBET award No. 1947303.

Appendix A. Supplementary data

Supplementary data associated with this article can be found, in the online version, at https://doi.org/10.1016/j.jcou.2021.101642.

References

[1] R.B. Jackson, E.I. Solomon, J.G. Canadell, M. Cargnello, C.B. Field, Methane removal and atmospheric restoration, Nat. Sustain. 2 (6) (2019) 436–438.
[2] A. Bogaerts, X. Tu, J.C. Whitehead, G. Centi, L. Lefferts, O. Guaitella, F. Azzolina-Jury, H.-H. Kim, A.B. Murphy, W.F. Schneider, The 2020 plasma catalysis roadmap, J. Phys. D 53 (44) (2020), 443001.
[3] J. Shah, W. Wang, A. Bogaerts, M.L. Carreon, Ammonia synthesis by radio frequency plasma catalysis: revealing the underlying mechanisms, ACS Appl. Energy Mater. 1 (9) (2018) 4824–4839.
[4] J. Shah, T. Wu, J. Lucero, M.A. Carreon, M.L. Carreon, Nonthermal plasma synthesis of ammonia over Ni-MOF-74, ACS Sustain. Chem. Eng. 7 (1) (2018) 377–383.
[5] J. Shah, F. Gorky, P. Psarras, B. Seong, D.A. Gómez-Gualdrón, M.L. Carreon, Enhancement of the yield of ammonia by hydrogen-sink effect during plasma catalysis, ChemCatChem 12 (4) (2020) 1200–1211.
[6] J.R. Shah, F. Gorky, J. Lucero, M.A. Carreon, M.L. Carreon, Ammonia synthesis via atmospheric plasma catalysis: zeolite 5A, a case of study, Ind. Eng. Chem. Res. 59 (11) (2020) 5167–5176.
[7] M.L. Carreon, Plasma catalytic ammonia synthesis: state of the art and future directions, J. Phys. D 52 (48) (2019), 483001.
[8] J.R. Shah, J.M. Harrison, M.L. Carreon, Ammonia plasma-catalytic synthesis using low melting point alloys, Catalysts 8 (10) (2018) 437.
[9] F. Gorky, A. Best, J. Jasinski, B.J. Allen, A.C. Alba-Rubio, M.L. Carreon, Plasma catalytic ammonia synthesis on Ni nanoparticles: the size effect, J. Catal. 393 (2021) 369–380.
[10] F. Gorky, S.R. Guthrie, C.S. Smoljan, J.M. Crawford, M.A. Carreon, M.L. Carreon, Plasma ammonia synthesis over mesoporous silica SBA-15, J. Phys. D 54 (26) (2021), 264003.
[11] K. Yoshida, M. Okubo, T. Yamamoto, Distinction between nonthermal plasma and thermal desorptions for NO x and CO 2, Appl. Phys. Lett. 90 (13) (2007), 131501.
[12] S. Li, M. Ongis, G. Manzolini, F. Gallucci, Non-thermal plasma-assisted capture and conversion of CO2, Chem. Eng. J. 410 (2021), 128335.
[13] C. De Bie, J. Van Dijk, A. Bogaerts, The dominant pathways for the conversion of methane into oxygenates and syngas in an atmospheric pressure dielectric barrier discharge, J. Phys. Chem. C 119 (39) (2015) 22331–22350.
[14] D. Saha, Z. Bao, F. Jia, S. Deng, Adsorption of CO2, CH4, N2O, and N2 on MOF-5, MOF-177, and zeolite 5A, Environ. Sci. Technol. 44 (5) (2010) 1820–1826.
[15] A.G. Wong-Foy, A.J. Matzger, O.M. Yaghi, Exceptional H2 saturation uptake in microporous metal– organic frameworks, J. Am. Chem. Soc. 128 (11) (2006) 3494–3495.
[16] J.L.C. Rowsell, O.M. Yaghi, Strategies for hydrogen storage in metal–organic frameworks, Angew. Chem. Int. Ed. 44 (30) (2005) 4670–4679.
[17] A.R. Millward, O.M. Yaghi, Metal– organic frameworks with exceptionally high capacity for storage of carbon dioxide at room temperature, J. Am. Chem. Soc. 127 (51) (2005) 17998–17999.
[18] H.K. Chae, D.Y. Siberio-Perez, J. Kim, Y. Go, M. Eddaoudi, A.J. Matzger, M. O'Keeffe, O.M. Yaghi, A route to high surface area, porosity and inclusion of large molecules in crystals, Nature 427 (6974) (2004) 523–527.
[19] D. Saha, Z. Wei, S. Deng, Equilibrium, kinetics and enthalpy of hydrogen adsorption in MOF-177, Int. J. Hydrog. Energy 33 (24) (2008) 7479–7488.
[20] S.L. Yao, T. Takemoto, F. Ouyang, A. Nakayama, E. Suzuki, A. Mizuno, M. Okumoto, Selective oxidation of methane using a non-thermal pulsed plasma, Energy Fuels 14 (2) (2000) 459–463.
[21] P. Chawdhury, K. Bhargavi, C. Subrahmanyam, Enhanced synergy by plasma reduced Pd nanoparticles on in-plasma catalytic methane conversion to liquid oxygenates, Catal. Commun. 147 (2020), 106139.
[22] D.W. Larkin, L.L. Lobban, R.G. Mallinson, The direct partial oxidation of methane to organic oxygenates using a dielectric barrier discharge reactor as a catalytic reactor analog, Catal. Today 71 (1–2) (2001) 199–210.
[23] L.M. Zhou, B. Xue, U. Kogelschatz, B. Eliasson, Partial oxidation of methane to methanol with oxygen or air in a nonequilibrium discharge plasma, Plasma Chem. Plasma Process. 18 (3) (1998) 375–393.
[24] P. Chawdhury, Y. Wang, D. Ray, S. Mathieu, N. Wang, J. Harding, F. Bin, X. Tu, C. Subrahmanyam, A promising plasma-catalytic approach towards single-step methane conversion to oxygenates at room temperature, Appl. Catal. B 284 (2021), 119735.
[25] P. Chawdhury, D. Ray, T. Vinodkumar, C. Subrahmanyam, Catalytic DBD plasma approach for methane partial oxidation to methanol under ambient conditions, Catal. Today 337 (2019) 117–125.
[26] A. Indarto, Methanol synthesis from methane and oxygen with [Ga Cr]/Cu–Zn–Al catalyst in a dielectric barrier discharge, IONICS 20 (3) (2014) 445–449.
[27] A. Indarto, H. Lee, J.W. Choi, H.K. Song, Partial oxidation of methane with yttria-stabilized zirconia catalyst in a dielectric barrier discharge, Energy Sources Part A 30 (17) (2008) 1628–1636.
[28] D. Saha, S. Deng, Hydrogen adsorption on metal-organic framework MOF-177, Tsinghua Sci. Technol. 15 (4) (2010) 363–376.
[29] Y. Li, R.T. Yang, Gas adsorption and storage in metal– organic framework MOF-177, Langmuir 23 (26) (2007) 12937–12944.
[30] X. Li, F. Cheng, S. Zhang, J. Chen, Shape-controlled synthesis and lithium-storage study of metal-organic frameworks Zn4O (1, 3, 5-benzenetribenzoate) 2, J. Power Sources 160 (1) (2006) 542–547.
[31] M.L. Carreon, Plasma catalysis: a brief tutorial, Plasma Res. Express (2019) 043001.
[32] J. Cao, Y. Feng, S. Zhou, X. Sun, T. Wang, C. Wang, H. Li, Spatial aromatic fences of metal–organic frameworks for manipulating the electron spin of a fulleropyrrolidine nitroxide radical, Dalton Trans. 45 (28) (2016) 11272–11276.
[33] D. Saha, S. Deng, Structural stability of metal organic framework MOF-177, J. Phys. Chem. Lett. 1 (1) (2010) 73–78.
[34] J. Rowsell, Hydrogen Storage in Metal-Organic Frameworks: an Investigation of Structure-property Relationships, University of Michigan, 2005.
[35] F. Gorky, J.M. Lucero, J.M. Crawford, B. Blake, M.A. Carreon, M.L. Carreon, Plasma-induced catalytic conversion of nitrogen and hydrogen to Ammonia over zeolitic imidazolate frameworks ZIF-8 and ZIF-67, ACS Appl. Mater. Interfaces (2021).
[36] Y. Feng, T. Wang, Y. Li, J. Li, J. Wu, B. Wu, L. Jiang, C. Wang, Steering metallofullerene electron spin in porous metal–organic framework, J. Am. Chem. Soc. 137 (47) (2015) 15055–15060.
[37] R. Vakili, R. Gholami, C.E. Stere, S. Chansai, H. Chen, S.M. Holmes, Y. Jiao, C. Hardacre, X. Fan, Plasma-assisted catalytic dry reforming of methane (DRM) over metal-organic frameworks (MOFs)-based catalysts, Appl. Catal. B 260 (2020), 118195.
[38] L. Wang, Y. Yi, H. Guo, X. Tu, Atmospheric pressure and room temperature synthesis of methanol through plasma-catalytic hydrogenation of CO2, ACS Catal. 8 (1) (2018) 90–100.
[39] R. Guil-López, N. Mota, J. Llorente, E. Millán, B. Pawelec, J.L.G. Fierro, R. M. Navarro, Methanol synthesis from CO2: a review of the latest developments in heterogeneous catalysis, Materials 12 (23) (2019) 3902.
[40] K. Yoshida, Characteristics of the desorption of NOx from Mn-Cu mixed oxide induced by non-thermal plasma, Int. J. Plasma Environ. Sci. Technol. 12 (1) (2018) 1–6.
[41] A.M. Varghese, G.N. Karanikolos, CO2 capture adsorbents functionalized by amine–bearing polymers: a review, Int. J. Greenh. Gas Control. 96 (2020), 103005.
[42] I. Sreedhar, T. Nahar, A. Venugopal, B. Srinivas, Carbon capture by absorption–path covered and ahead, Renew. Sustain. Energy Rev. 76 (2017) 1080–1107.
[43] A. Samanta, A. Zhao, G.K.H. Shimizu, P. Sarkar, R. Gupta, Post-combustion CO2 capture using solid sorbents: a review, Ind. Eng. Chem. Res. 51 (4) (2012) 1438–1463.
[44] J. Wang, L. Huang, R. Yang, Z. Zhang, J. Wu, Y. Gao, Q. Wang, D. O'Hare, Z. Zhong, Recent advances in solid sorbents for CO2 capture and new development trends, Energy Environ. Sci. 7 (11) (2014) 3478–3518.
[45] P. Gulati, U.N. Pal, M. Kumar, R. Prakash, V. Srivastava, V. Vyas, Diagnostic of plasma discharge parameters in helium filled dielectric barrier discharge, J. Theor. Appl. Phys. 6 (1) (2012) 1–8.
[46] P. Chawdhury, D. Ray, C. Subrahmanyam, Single step conversion of methane to methanol assisted by nonthermal plasma, Fuel Process. Technol. 179 (2018) 32–41.
[47] Jun-Feng Z, Xin-Chao Bian, Qiang Chen, Fu-Ping Liu, Zhong-Wei, Diagnosis of methane plasma generated in an atmospheric pressure DBD micro-jet by optical emission spectroscopy, Chin. Phys. Lett. 26 (3) (2009), 035203.
[48] L. Wang, Y. Yi, C. Wu, H. Guo, X. Tu, One-step reforming of CO2 and CH4 into high-value liquid chemicals and fuels at room temperature by plasma-driven catalysis, Angew. Chem. Int. Ed. 56 (44) (2017) 13679–13683.
[49] M. Kraus, W. Egli, K. Haffner, B. Eliasson, U. Kogelschatz, A. Wokaun, Investigation of mechanistic aspects of the catalytic CO2 reforming of methane in a dielectric-barrier discharge using optical emission spectroscopy and kinetic modeling, Phys. Chem. Chem. Phys. 4 (4) (2002) 668–675.